

Effect of gamma radiation in undoped SnO₂ thin films

A. F. Maged*, L. A. Nada and M. Amin^a

National Center for Radiation Research and Technology, (NCRRT),
Atomic Energy Authority, P. O. Box 29, Nasr City, Cairo, Egypt

^aCairo University, Faculty of Science, Giza, Egypt

* Corresponding author. Tel/Fax: 0202 22749298

Email: magedali@hotmail.com

Abstract

This paper was reported on study the effect of gamma radiation on nanoporous SnO₂ electrodes for dye-sensitized solar cells. Structural, optical and electrical properties were studied. The refractive index was decreased with the increase in gamma radiation. The resistivity of thin films was decreased about 40% with the increase of gamma radiation at 659 nm film thicknesses. The mobility and carrier concentration were increased with the increase of gamma dose at 659 nm film thickness.

Key words: SnO₂; semiconductors; thin film; radiation

1. Introduction

Tin oxide has attracted great attention and many uses in recent decades because of its high transparency and conductivity combined with superior stability. The major applications of transparent conducting oxides include thin-film photovoltaic [1], gas sensors [2-5], optoelectronics [6], heat reflectors in solar cells windows [7]. The above-mentioned properties make them very useful in many fields of applications: transparent electrodes for silicon and SeTe and GeSeTe alloys [8]. The ionizing radiation is available especially as gamma, and determination of its effect is important for the efficient usage of devices on the satellites, space shuttles and industrial Cobalt units [9]. Glass materials are broadly used in the application areas of low-orbit satellites and spacecrafts [10]. Therefore, examination of radiation effects on the glass materials is imperative as well. These effects are associated with the energy of radiation, as well as the total dose [11].

2. Experimental procedure

2.1 Spray pyrolysis was a physical deposition technique where the endothermic thermal decomposition was taken place at the hot surface of the substrate to give the final product. The nano-structured films were prepared from crystalline hydrate of tin tetrachloride (SnCl₄.5H₂O) which had weight of 5gm by dissolution in 5mL pure methanol. The substrate temperature was in the range of 400–500°C. After the deposition, the films were dried for 1 hour at room temperature. The film thickness

was estimated from UV-Vis spectrophotometer, and found 191, 232, 478 and 659 nm, respectively. The deposited thin films were confirmed by X-ray diffraction examination using an X-ray diffractometer Shimadzu machine model (XD-DI series) with Cu-K α radiation as a target, $\lambda=1.548 \text{ \AA}$, operated at 400 kV and 30 mA using Bragg–Brentano method. The average crystallite size was estimated from the width of x-ray lines by Scherrer's method. The optical transmittance spectra of SnO₂ films were measured in the wavelength range from 190 to 1100 nm by means of the Specord 210 plus UV-Vis spectrophotometer. The electrical properties were studied by sheet resistance method by using RCL meter at room temperature (The Philips / Fluke PM6303A RCL Meter). All measurements were made using a 4-wire technique, which ensures high-accuracy measurements, even for low-impedance components. SnO₂ films were exposed to a Co-60 gamma-radiation source with a dose rate 2.32 kGy. hr⁻¹ at room temperature in National Center for Radiation Research and Technology, Egyptian Atomic Energy Authority. The selection of exposure dose was in the range 0.5-22 kGy which is based on industrial applications.

3- Result and discussion

3-1 X-ray analysis

It was seen that the pattern of the SnO₂ film with diffraction peaks at about positions 26.8, 35.3, 37.4, and 52.4 degree, correspond to diffraction signals produced by the (110), (101), (200) and (211) crystalline planes of the tetragonal structure of Tin element. These peaks were increased with the increase of thickness at same positions as shown in Fig (1). It may be due to the intensity of the diffraction peaks were determined by the arrangement of atoms in the entire crystal.

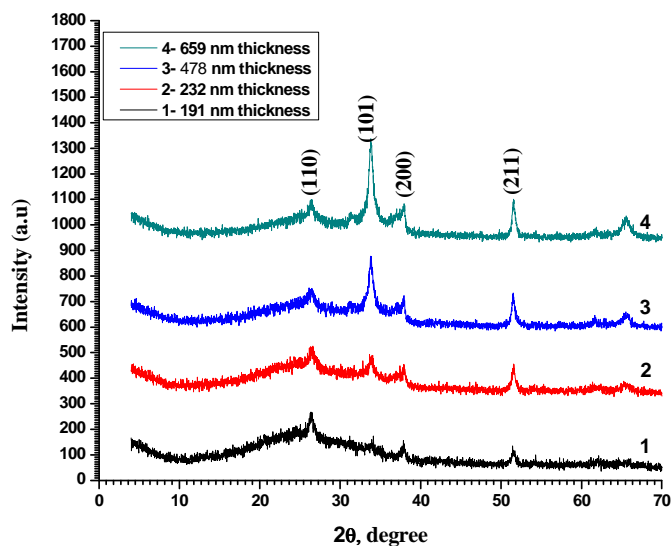


Fig. 1 Plot of x-ray diffraction spectrum at all thicknesses before gamma radiation

It was observed that no change in the peak intensity and position after exposing to gamma radiation up to 22 kGy as shown in **Fig. (2)**.

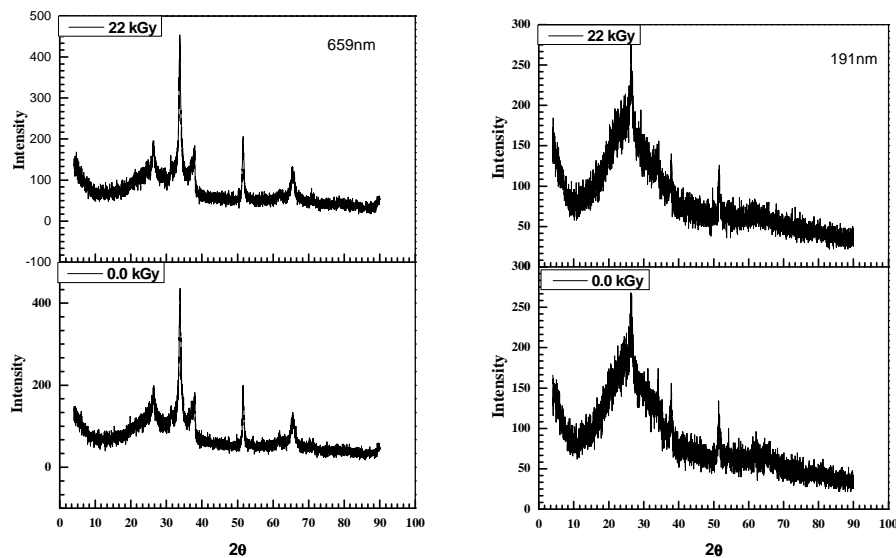


Fig. 2 Plot of x-ray diffraction spectrum at 659 and 191 nm film thicknesses before and after gamma radiation

Assuming a homogeneous strain across crystallites, the crystallite size of nano-crystallite was calculated from the full width half maximum (FWHM) values by using the Scherrer formula for crystallite size broadening of diffraction peaks,

$$D = \frac{0.9 \lambda}{B \cos \theta} \quad (1)$$

where D is crystallite size, λ is the wavelength of x-ray, B is FWHM of diffraction peak and θ is the diffraction angle. The crystallite size of tin oxide thin film thickness of 191, 232, 478 and 659 nm were found to be 8, 8, 9 and 16 nm.

3-2 Theoretical background of optical transition

Basically, there are two types of optical transition that can occur at the fundamental edge of crystalline semiconductors: direct and indirect transitions. For simple parabolic bands ($N(E) \propto E^{1/2}$) and for direct transitions,

$$\alpha(\nu) n_0 h\nu \approx (h\nu - E_g)^n \quad (2)$$

Where, α is the absorption coefficient, n is a constant of $1/2$ for allowed transitions and of $3/2$ for forbidden transitions in the quantum-mechanical sense, n_0 is the refractive index which is assumed to be a constant over energy variation, $h\nu$ is photon energy and E_g is the band gap energy of the material under investigation. This type of absorption is independent of temperature apart from any variation in E_g .

3-3 Optical absorption shift:

There is α shift in the band gap towards higher energy for the thin film having higher carrier density. This shift was due to the filling of the states near the bottom of the conduction band [12-13]. The shift was given by the relation,

$$E_g = E_{g0} + \Delta E_g^{BM} \quad (3)$$

where E_{g0} is the intrinsic band gap and ΔE_g^{BM} is the BM shift (Burstein- Moss shift).

The shift is related to the carrier density as,

$$\Delta E_g^{BM} = \frac{\pi^2 \hbar^2}{2m^*} \left(\frac{3N}{\pi} \right)^{2/3} \quad (4)$$

where m^* is the reduced effective mass and N is carrier density.

3-4 Optical band gap

The direct transition property of SnO₂ films, Eq.2 was applied with $n = 1/2$ in the case of the crystalline film, and with $n = 2$ which could be applied to amorphous film [8]. The optical properties mainly depend on the refractive index of the material and thickness of the film. The absorption and dispersion of a plane electromagnetic wave

was described by the complex refractive index $\hat{N} = n + ik$, where n is the real refractive index and k is the extinction coefficient. The physical significance of k is that on traversing a distance in the medium equal to one vacuum wavelength, the amplitude of the wave decreases by the factor $\exp(-2\pi ik)$. It was observed that the decrease in the transmission with the increase in thin film thicknesses. **It may be due to the increase of opacity as shown in Fig. (3).**

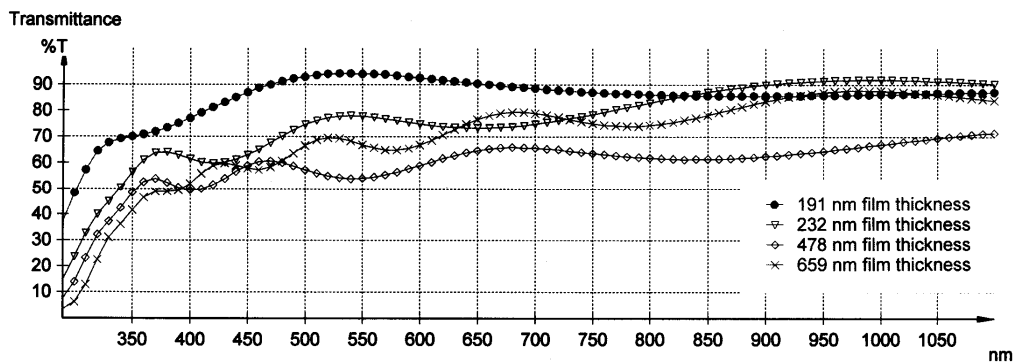


Fig. 3 Plot of transmission % as a function of wavelength for SnO₂ film of different thicknesses.

The transmission spectra of glass substrate (**corning glass**) and as deposited before and after gamma radiation **exposure** were shown in Fig. 4.

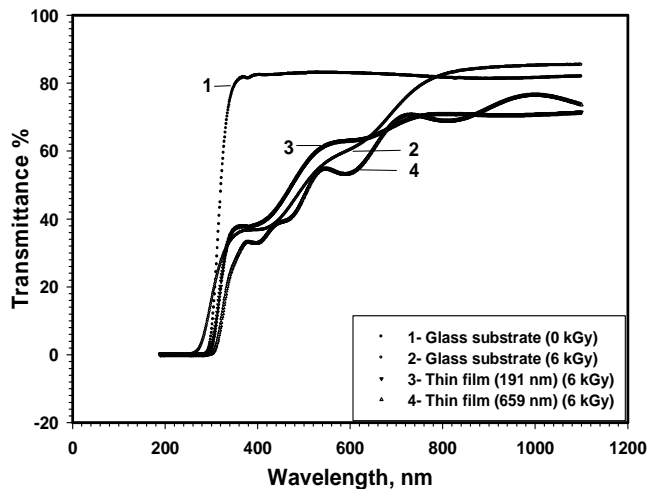


Fig. 4. Transmission spectra of glass substrate and as deposited films before and after gamma radiation.

It was noticed that a decrease 63% in transmission for the glass substrate after gamma radiation exposure **in visible range**. This decrease might be due to that the transparent

glass was converted into brown color after exposing to 6 kGy gamma dose. There was absorption coefficient, α shift at absorption edge towards higher energy with the increase of film thicknesses as shown in Fig. 5.

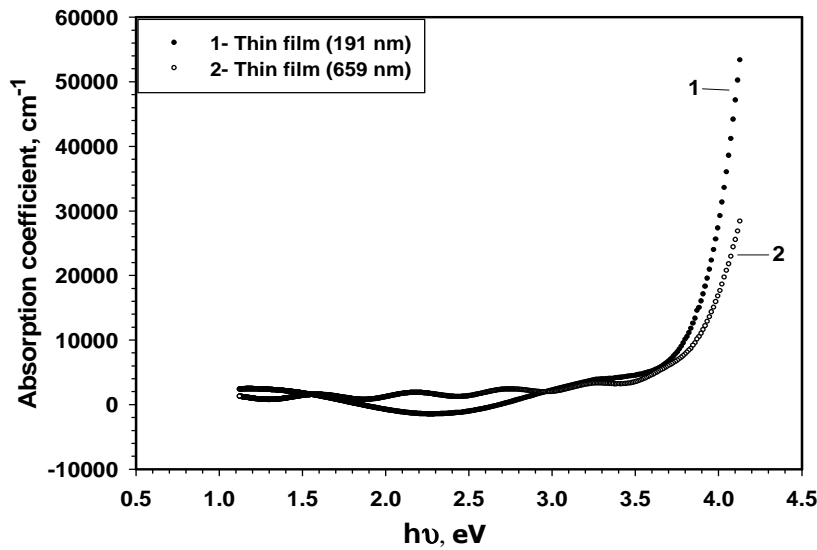


Fig. 5 Plot of absorption coefficient α vs. energy for SnO₂ at 191 and 659 nm films thickness, respectively.

The absorption coefficient difference (δ) as a function of gamma dose for SnO₂ at 191 nm film thickness was shown in Fig.6. There was an exponentially increase up to gamma dose 6 kGy then it was saturated. It could be possible to use as gamma dosimeter up to 6 kGy which is used in the industrial applications.

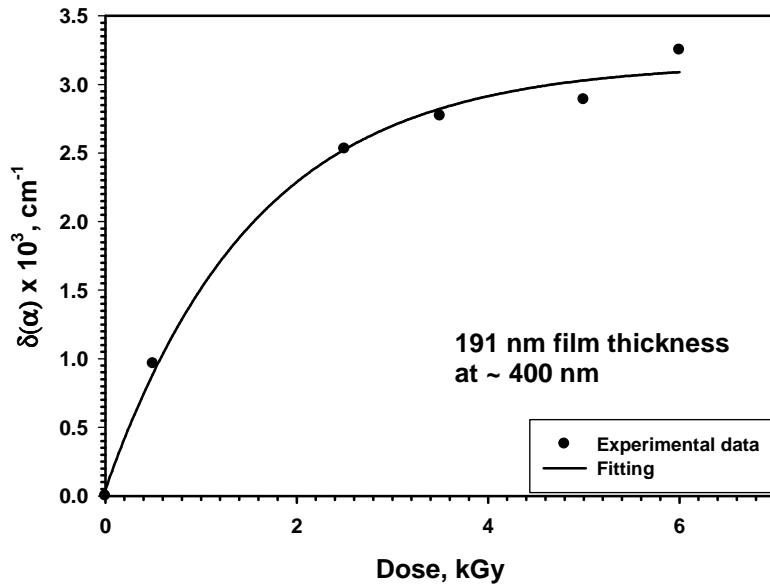


Fig. 6 Absorption coefficient difference (δ) as a function of gamma dose of selected film.

The absorption coefficient, α , as a function of wavelength for SnO_2 at 659 nm film thickness in the interference area was shown in **Fig.7**. There was an increase in the absorption coefficient with the increase in wavelength and more increase after gamma radiation. The absorbance as a function of wavelength in the interference area before radiation (**Fig.7-1**) has different orientation behavior from the radiated sample (**Fig.7-2**). It might be due to the color change of glass substrate after exposing to gamma radiation. The same behavior of (α) was observed to the extinction coefficient (k).

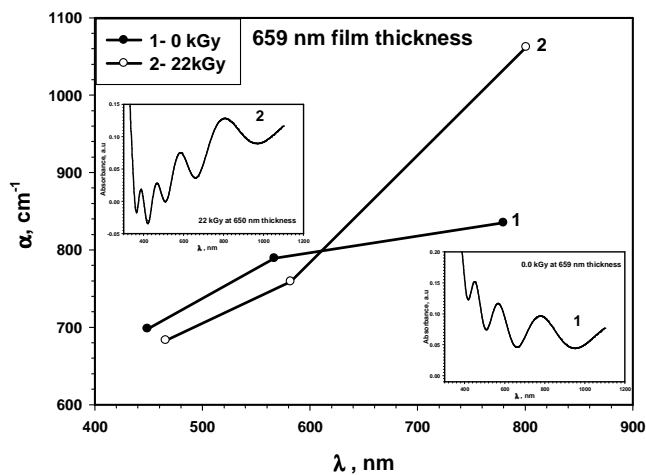


Fig. 7 The absorption coefficient, α vs. wavelength in the interference area of film before and after radiation.

The refractive index was decreased with the increase of wavelength before and after radiation exposure as shown in Fig. 8. The refractive index and extinction coefficient for the thin film at thickness range 191-659 nm were calculated in the interference area. The refractive index in this study was coincidence with atomic layer deposition method of tin oxide films [14]. The absorbance as a function of wavelength before and after radiation exposure was shown in Fig. 8 (1 and 2).

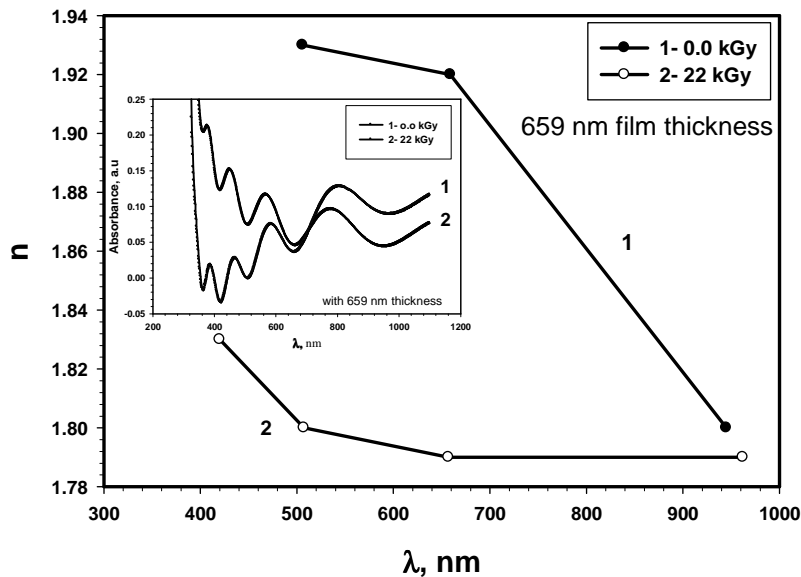


Fig. 8 The refractive index vs. wavelength in interference area of film before and after radiation.

Our results were relatively matching the changes in the refractive index correspond to the fact that the refractive indices of SnO₂ were 1.96 and 1.79 before and after gamma radiation exposure, respectively [14-15]. The values of k were in the range of 1.6×10^{-2} - 1.8×10^{-2} before radiation and it was found in the range 0.3×10^{-2} - 3.2×10^{-2} after radiation exposure. As reported in [16] the refractive index of SnO₂ at 550 nm is 2.0 and the extinction coefficient was 0.03 and these results were relatively consistent to this work. The high absorption coefficient was observed for the SnO₂ films due to the polycrystalline of the sample, which was evident from the x-ray studies.

The direct band gap of tin oxide were reported 4.3 eV [17], 3.1 eV [18] and 3.95 eV [19]. In the present report, the direct band gap obtained was 3.88 eV at an atmospheric pressure of 1.01×10^{-5} Pa and room temperature before radiation and 3.96 after radiation exposure. The variation of the direct band gap with radiation for 191 and 659 nm film thicknesses were may be due to the Burstein-Moss shift.

3-5 Electrical properties

It was found that the sheet resistance decreased from $16 \text{ k}\Omega/\square$ to $3 \text{ k}\Omega/\square$ with the increase of film thickness. The resistivity was decreased from $32 \times 10^{-2} \Omega\text{-cm}$, to $12 \times 10^{-2} \Omega\text{-cm}$ after radiation for 191 nm film thickness. It was found that the resistivity decreased exponentially with the increase gamma dose and it might be used as gamma dosimeter. The mobility and carrier concentration were found $1.1 \text{ cm}^2/\text{V-s}$ and $1.9 \times 10^{19}/\text{cm}^3$, respectively before radiation at 191 nm film thickness. These values were found relatively consistent with the values was reported [14-15]. The mobility and carrier concentration were increased with the increase of radiation at 659 nm film thickness and it is believed that damage caused to the contact regions is responsible for this shift. Ionization is the process of removing or adding an electron to a neutral atom, thereby creating an ion.

Conclusion

The structural, optical and electrical properties of SnO_2 thin films on glass substrates were evaluated before and after gamma radiation exposure. X-ray diffraction was revealed that the SnO_2 films were crystalline. A red shift in the absorption edge was observed with the increase of thickness. The thin film deposited on glass was yielded optical transmission of 94% at 191 nm film thickness. The optical energy gap was increased to 3.95 eV at gamma dose 6 kGy. There was absorption coefficient, α shift in the band gap towards higher energy for the thin film which having higher carrier density. At wavelength range 400–950 nm, the values of extinction coefficient were in the range of 1.6×10^{-2} – 1.8×10^{-2} before radiation and it was found in the range 0.3×10^{-2} – 3.1×10^{-2} after radiation exposure. Radiation was induced changes in the optical and electrical properties of SnO_2 films resulted in the degradation of their performance.

Acknowledgments

Special thanks are due to Solid State and Electron Accelerator Department Staff members, EAEA, for their help of this work.

References

- [1] Stefik M, Heiligtag F. J., Niederberger M., and Grätzel M. 2013. *ACS Nano*, 7 (10), 8981–8989.
- [2] Huang X. J., Choi Y. K., Yun K. S., and Yoon E. 2006. *Sensors and Actuators B* 115, 357.
- [3] Yang H. M., Zhang X. C., and Tang A. D. 2006. *Nanotechnology* 17, 2860.
- [4] Simakov V., Yakusheva O., Grebennikov A., and Kisin V. 2006. *Sensors and Actuators B* 116, 221.
- [5] Jin C. J., Yamazaki T., Ito K., Kikuta T., and Nakatani N. 2006. *Vacuum* 80, 723.

- [6] Wang G. F., Tao X. M., and Huang H. M. 2005. *Coloration Technology* 121, 132.
- [7] Maghanga A., Niklasson G. G., Granqvist C., and Mghendi M. 2011. *Applied Optics*, 50, 19 /1.
- [8] Maged A.F., Amin G.A.M., Semary M, E. Borham 2010. *Thin Solid Films* 518, 2628–2631.
- [9] Bhata J.S., Maddani K.I. , Karguppikar A.M., Ganesh S. 2007. *Nuclear Instruments and Methods in Physics Research B* , 258(2), 369–374.
- [10] Maged A.F, Montasser K.I. and Amer H.H. 1998. *J. Materials Chemistry and Physics*, 56/2,184-188.
- [11] Goswami A. 2003. *Thin Film Fundamentals*, New Age International (P) Limited, Publishers, New Delhi.
- [12] Burstein E. 1954. *Physical Review*, 93, 632–633.
- [13] Moss T. S. 1954. *Proceedings of the Physical Society B*, 67, 775–782.
- [14] Elam W. J., Baker A. D , Hryn J. A., Martinson B. F. A., Pellin J. M., Hupp T. J. 2008. *Journal of Vacuum Science & Technology A*, 26(2) 244–252.
- [15] Heo J., Hock A. S., and Gordon R. G. 2010. *Chemistry of Materials*, 22, 4964–4973.
- [16] Habibi M. H., Talebian N. 2005. *Acta Chimica Slovenica* 52, 53.
- [17] Spence W. 1967. *Journal of Applied Physics*, 38, 3767.
- [18] Reddy M. H. M. and Chandorkar A. N. 1999. *Thin Solid Films*, 349, 260.
- [19] Sundaram K.B. and Bhagavat G.K. 1981. *Journal of Physics D: Applied Physics*, 14, 921.